PROCEEDINGS OF SCIENCE

Interpolating the ‘t Hooft model between Instant and Light-Front dynamics in the Coulomb Gauge

Hunter Duggin,[a,*] **Chueng-Ryong Ji**[a] **and Bailing Ma**[b]

[a] *Department of Physics, North Carolina State University, 2401 Stinson Dr, Raleigh NC, U.S.*

[b] *Argonne National Laboratory, Lemont, Illinois 60439, USA*

E-mail: hpduggin@ncsu.edu, crji@ncsu.edu, mab@anl.gov

The 1+1D model of quantum chromodynamics (QCD) in the infinite number of colors, or ’t Hooft model, can be interpolated between the instant form dynamics (IFD) and the light-front dynamics (LFD) using an interpolation parameter 0 (IFD) $\leq \delta \leq \pi/4$ (LFD). This was realized in the interpolating axial gauge which links the axial gauge ($A^1 = 0$) in IFD and the light-front gauge ($A^+ = 0$) [1]. In this presentation, we discuss the corresponding realization in the interpolating Coulomb gauge which links the temporal gauge ($A^0 = 0$) in IFD and the light-front gauge ($A^+ = 0$) and its benefit of resolving the issue associated with the absence of the conjugate field to the gauge field A^0 in the axial gauge. In both gauges, all degrees of freedom are physical making these gauge choices ideal for finding the bound-state equations and for renormalizability. Although the gauge independence of the physical observables such as the meson mass spectra following Regge trajectories may be guaranteed due to the gauge symmetry of QCD, the realization and interpretation of the identical physical results may depend on the gauge choices. Here, we discuss such difference in the realization of the confinement phenomena *à la* linear potential in the two different gauges, Coulomb vs. Axial, and highlight the gauge independent physical results expected. We also comment on the utility of the interpolation which leads to an alternative quasi-PDF that can be implemented in the lattice QCD without suffering from the large momentum boost.

25th International Spin Physics Symposium (SPIN 2023)
24-29 September 2023
Durham, NC, USA

*Speaker

PoS(SPIN2023)051

1. Introduction

The three forms of Hamiltonian dynamics, those being the IFD, LFD, and point form dynamics, were first proposed by Dirac in 1949 [2]. Only in recent times, however, have we begun to connect the popular IFD and LFD through interpolation. The LFD in particular has the characteristic of having the maximum number of seven kinematic operators out of the ten Poincare operators. This unique feature of the LFD saves a large amount of dynamical effort when computing physical quantities, making the LFD an ideal choice for the hadron physics. Through the interpolation method, it can be clearly shown how the longitudinal boost operation becomes kinematic when the dynamic form approaches the LFD [3].

In order to link the two forms of dynamics, and to make use of the symmetry advantages found in the light front along with the familiarity of the instant form, we introduce the interpolating dynamics between the IFD and the LFD. We rotate the space-time axes of the instant form by a continuous parameter δ called as the interpolation angle. The interpolation angle, δ, runs from 0 to

$$\begin{bmatrix} x^{\hat{+}} \\ x^{\hat{-}} \end{bmatrix} = \begin{bmatrix} \cos\delta & \sin\delta \\ \sin\delta & -\cos\delta \end{bmatrix} \begin{bmatrix} x^0 \\ x^1 \end{bmatrix}$$

$\frac{\pi}{4}$. The lower index variables $x_{\hat{+}}$ and $x_{\hat{-}}$ are related to the upper ones by $x_{\hat{+}} = g_{\hat{+}\hat{+}}\, x^{\hat{+}} + g_{\hat{+}\hat{-}} x^{\hat{-}} = \mathbb{C}x^{\hat{+}} + \mathbb{S}\, x^{\hat{-}}$ where the shorthand notations are defined by $\mathbb{C} = \cos 2\delta$ and $\mathbb{S} = \sin 2\delta$. All the indices with the hat-notation signify the variables with the interpolation angle δ, and when $\delta = \frac{\pi}{4}$ specifically, the variables coincide with those in the LFD without the hat-notation. When $\delta = 0$ we recover the ordinary IFD. By varying the parameter δ and studying the limiting behavior when δ approaches $\frac{\pi}{4}$, we can trace the fate of symmetry properties, Poincare operators, vacuum structure, as well as calculations of physical processes such as scattering amplitudes [4]. Recent comprehensive review on the topics of the interpolation between the IFD and the LFD can be found in Ref.[5]. With the interpolation approach, we clear up the prevailing confusion of a particular reference frame with a quantization form (where the degrees of freedom are changed due to the change of the "time" variable). In particular, we remove the confusion of the Infinite Momentum Frame (IMF) in equal-time dynamics with the LFD. Both formulations, IMF and LFD, have the property that the contributions of backward propagating time-ordered diagrams tend to vanish. However, in IMF the time-ordering is done with ordinary time, while in LFD the ordering is by light-front time. The LFD has the property of boost invariance, i.e., the amplitude of a time-ordered diagram does not change no matter what reference frame is taken, while the IMF result is only valid when the particles involved are boosted to the infinite momentum. We emphasize that IMF and LFD are distinctively different from each other.

The two dimensional model of quantum chromodynamics (QCD_2) with the number of colors $N_c \to \infty$ has continually served its purpose as an elementary tool to understand strong interactions. Under this large N_c approximation using a $1/N_c$ expansion, 't Hooft showed that the non-planar diagrams vanish. Thus, for example, only the rainbow diagrams need to be summed over when computing the self mass of the quark. 't Hooft originally postulated this model in the light-front dynamics in his seminal paper [6]. Some time later, Bars and Green re-derived it using the standard

Instant Form Dynamics (IFD) [7]. The interpolation of the 't Hooft model between the IFD and the LFD was made previously in [1].

Both the IFD and interpolating dynamics calculations were done using the axial gauge condition ($A^1 = 0$ for the IFD and $A_{\hat{-}} = 0$ for interpolating dynamics). In the axial gauge, however, the gauge field A^0 is not fixed but arbitrary due to the absence of its conjugate field, namely $\pi^0 = 0$. In most general case, the corresponding field strength tensor associated with the gauge field A^0, i.e. $E^1 = -\partial^1 A^0$ is not fixed. As discussed in [7], however, one may not concern this issue for the physical states of interest such as the color singlet states in QCD or the charge neutral states in QED. Nevertheless, in order to combat this issue associated with $\pi^0 = 0$, one may impose a gauge condition that fixes the A^0 field. The Coulomb gauge $\partial^1 A^1 = 0$ is equivalent to the temporal gauge $A^0 = 0$ by fixing the initial gauge field A^0 to be zero, and thus the Coulomb gauge avoids the issue associated with $\pi^0 = 0$ once and for all. Moreover, it was shown that the Coulomb gauge in 1+1 D naturally provides the confining potential independent of charge [8]. However, this finding in the Coulomb gauge was made only in the IFD but not yet linked to the LFD. Thus, it motivates us to interpolate the Coulomb gauge between the IFD and the LFD in the analysis of the 't Hooft model. We have previously interpolated QED in 3+1 D between the IFD and the LFD using the interpolating Coulomb gauge and demonstrated that it links the Coulomb gauge $\vec{\nabla} \cdot \vec{A} = 0$ in the IFD and the light-front gauge $A^+ = 0$ in the LFD [9]. In 1+1 D, the interpolating Coulomb gauge $\partial_{\hat{-}} A_{\hat{-}} = 0$ links the Coulomb gauge $\partial^1 A^1 = 0$ in IFD and the light-front gauge $A^+ = 0$ in LFD. Calculations for the linear confining potential in the Coulomb gauge have been done in the IFD [8]. In order to resolve the $\pi^0 = 0$ issue, we may rederive the charge independent interpolating potential in the interpolating Coulomb gauge ($A^{\hat{+}} = 0$), link this to the light-front gauge ($A^+ = 0$), and then realizing the unique characteristic relationship in the light-front gauge, namely $A^+ = A_-$ $= 0$, we utilize the interpolating axial gauge ($A_{\hat{-}} = 0$) to reach the the axial gauge ($A^1 = 0$) in IFD which was problematic due to the $\pi^0 = 0$ issue. We hope to investigate this further in the 't

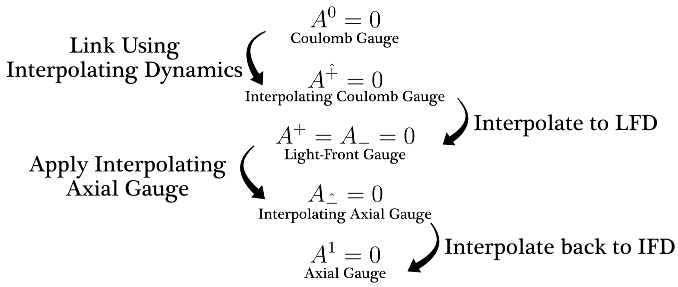

Figure 1: Illustrative representation of the proposed $\pi^0 = 0$ resolution

Hooft model and show that the physical quantities such as the mass gap, bound state spectroscopy, etc. remain unchanged in this specific route of sequencing both interpolating Coulomb gauge and interpolating axial gauge. We also note that the interpolating dynamics can lead to an alternative quasi-PDF that is not only dependent on the momentum, but also on the interpolation parameter δ. These alternative quasi-PDFs can be implemented into the lattice QCD and would not suffer from the large momentum boost.

2. Interpolating Coulomb Gauge

In analyzing models such as the 't Hooft model, one must specify the choice of gauge. Much like the axial gauge found in [1] and [7], the Coulomb gauge is ghost free, and is convenient to use for renormalizability [10]. To illustrate the $\pi^0 = 0$ issue discussed in the introduction we take the Canonical commutation relations.

The conjugate fields π_0 to the field A_0 is defined as

$$\pi_0\left(x^0, x^1\right) = \frac{\partial \mathcal{L}}{\partial\left[\partial_0 A_0\left(x^0, x^1\right)\right]} \tag{1}$$

in the IFD. At first glance, this seems rather standard. However, it is interesting to note what happens when the interpolating axial gauge condition is applied to the gauge fields. Since no term containing $\partial_0 A^0$ appears in $\mathcal{L}$ [1], the gauge field is only dependent on the space dimension x^1. The canonical variables are time dependent, implying that the gauge field is not fixed. In other words, using equation (1), we determine $\pi^0 = 0$ since no $\partial_0 A^0$ term appears in $\mathcal{L}$. This makes the definition of the gauge field A^1 ambiguous. The way to navigate around this ambiguity is to use the equation of motion for the gauge field as a constraint and derive the field. This comes at the cost of an added space dependent function term (called F in [1]), which cannot be specified. In this case, the on-mass-shell pole disappearing in the dressed quark propagator is interpreted to be confinement.

Adjacently, it can be shown that the Coulomb gauge gives rise to a confining potential that is independent of the charge [8]. In IFD, this looks like

$$\partial_1 A_1 = 0 \implies \partial^0 A^0 = 0. \tag{2}$$

Because this is a first order differential equation, we have the freedom to pick an initial condition. Thus, we choose the simplest case, being $A^0 = 0$ once and for all. Interestingly, one can see that the gauge has become fixed, and the conjugate field is now able to be found explicitly using equation (1). We can define the conjugate field as the electric field $E = -\partial_0 A^1$. From Gauss's law, we define a Gauss operator G [8].

$$G(x^0, x^1)|phys>= [\partial_1 E(x^0, x^1) - e\psi^\dagger\psi(x^0, x^1)]|phys>= 0 \tag{3}$$

Which when applied to a physical state will give zero because physical states are invariant under time independent gauge transformations, provided they are annihilated by their generator. Solving this, one can define an operator for the field E to be

$$E(x^0, x^1) = \partial_1 \int dy \left[\kappa x^1 y + \frac{e}{2}|x^1 - y|\psi^\dagger\psi\right] \tag{4}$$

Using this, one can find the Hamiltonian and solve for the potential as explored in [8] to obtain a linear potential, where the slope is dependent on the initial and boundary conditions imposed when applying the Gauss operator to a physical state. One can follow the same steps described above in the interpolating dynamics, where the IFD can be linked to the LFD description with the light-front gauge $A^+ = 0$ using the interpolating Coulomb gauge, effectively $A^{\hat{+}} = 0$.

PoS(SPIN2023)051

Taking the LFD limit ($\delta \to \frac{\pi}{4}$) in the interpolating Coulomb gauge yields effectively the light-front gauge condition

$$A^{+} = A_{-} = 0. \tag{5}$$

Then, we interpolate the $A_{-} = 0$ condition to get the interpolating axial gauge $A_{\hat{-}} = 0$ and ultimately obtain the result of the axial gauge in the IFD limit ($\delta \to 0$). This procedure illustrated in Fig.1 resolves the $\pi^0 = 0$ problem in the IFD when using the axial gauge, and both are connected by the light-front gauge. All of this aside, the 't Hooft model respects local gauge invariance. While the intermediate steps in calculating physical quantities will be different, we expect physical results to be independent of the gauge and interpolation parameter δ. Proceeding forward, we briefly summarize a few results obtained using the interpolation axial gauge in [1] and expect their gauge independence.

3. Expected Mass Gap

Similar to the work of Bars and Green in [7], we can write down the mass gap equation, noting that in the kernel, only the planar diagrams are summed over because of the large N_c condition.

$$\Sigma\left(p_{\hat{-}}\right) = i\frac{\lambda}{2\pi}\int \frac{dk_{\hat{-}}dk_{\hat{+}}}{\left(p_{\hat{-}} - k_{\hat{-}}\right)^2}\gamma^{\hat{+}}\frac{1}{\not{k} - m - \Sigma\left(k_{\hat{-}}\right) + i\epsilon}\gamma^{\hat{+}} \tag{6}$$

and we write down the quark self interaction as

$$\Sigma\left(p_{\hat{-}}\right) = \sqrt{\mathbb{C}}A\left(p_{\hat{-}}\right) + \gamma_{\hat{-}}B\left(p_{\hat{-}}\right) \tag{7}$$

We want to fix the angle θ. Such that

$$\theta = \theta_b + \theta_f \tag{8}$$

where θ_b is the Bogoliubov angle. When added to the angle found in the free case θ_f, we obtain the angle in the general case.

Using these equations, we can determine the mass gap equation to be

$$E\left(p_{\hat{-}}\right) = p_{\hat{-}}\sin\theta\left(p_{\hat{-}}\right) + \sqrt{\mathbb{C}}m\cos\theta\left(p_{\hat{-}}\right) + \frac{\lambda}{2}\int\frac{dk_{\hat{-}}}{\left(p_{\hat{-}} - k_{\hat{-}}\right)^2}\cos\left(\theta\left(p_{\hat{-}}\right) - \theta(k_{\hat{-}})\right) \tag{9}$$

One can visualize eq. (9) geometrically using Figure 2. Now, we can rescale the interpolating mass gap equation using the wave function renormalization factor $F\left(p_{\hat{-}}\right)$ and the mass function $M\left(p_{\hat{-}}\right)$ to get

$$\frac{F\left(p'_{\hat{-}}\right)E\left(p'_{\hat{-}}\right)}{\sqrt{\mathbb{C}}} = \sqrt{\left(M\left(p'_{\hat{-}}\right)\right)^2 + p^{2'}_{\hat{-}}} := \tilde{E}\left(p'_{\hat{-}}\right) \tag{10}$$

where $p'_{\hat{-}} = \frac{p_{\hat{-}}}{\sqrt{\mathbb{C}}}$. We can also easily see the familiar relativistic energy-momentum relation in terms of these rescaled variables given by

$$\tilde{E}^2\left(p'_{\hat{-}}\right) = M^2\left(p'_{\hat{-}}\right) + p^{'2}_{\hat{-}} \tag{11}$$

This angle $\theta = \theta_f + \theta_b$ remains unchanged under re-scaling from E to $\tilde{E}$, but the lengths of the legs will change. The solution of equation (11) is plotted in Fig.2. Interestingly, the mass gap is found to be independent of interpolation angle. Fig.3 highlights the constituent quark mass which can be used in the light front quark model phenomenology.

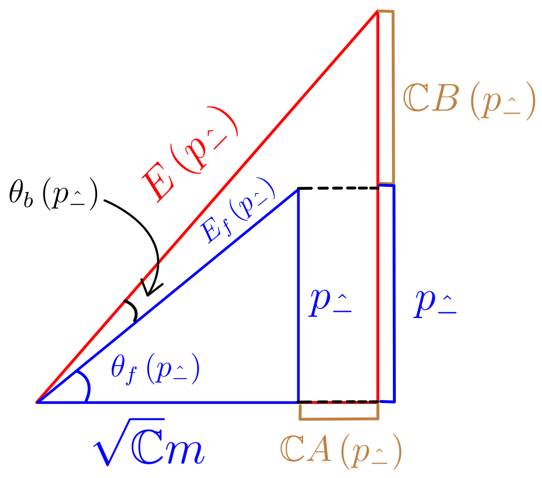

Figure 2: A geometric visualization of equation 10 (Axial Gauge)

4. Expected Bound State

After solving the single body mass gap equation, we now discuss the bound-state problem. We write down the Bethe-Salpethe equation for the diagram shown in Fig.5 in [1], and after some derivation, we arrive at the following set of equations, where $\hat{\phi}_{\pm}\,(r^{\hat{-}}, x)$ are the two components of the mesonic wave function, representing the forward and backward motion of the quark-antiquark.

$$[-r^{\hat{+}}+E(xr^{\hat{-}})+E(r^{\hat{-}}-xr^{\hat{-}})]r^{\hat{-}}\hat{\phi}_+(r^{\hat{-}},x) = \lambda\mathbb{C}\int\frac{dy}{(x-y)^2}[C(x,y,r^{\hat{-}})\hat{\phi}_+\,(r^{\hat{-}},x)-S(x,y,r^{\hat{-}}\hat{\phi}_-\,(r^{\hat{-}},y)] \tag{12}$$

$$[r^{\hat{+}}+E(xr^{\hat{-}})+E(r^{\hat{-}}-xr^{\hat{-}})]r^{\hat{-}}\hat{\phi}_-(r^{\hat{-}},x) = \lambda\mathbb{C}\int\frac{dy}{(x-y)^2}[C(x,y,r^{\hat{-}})\hat{\phi}_-\,(r^{\hat{-}},y)-S(x,y,r^{\hat{-}}\hat{\phi}_+\,(r^{\hat{-}},x)]$$

where

$$C(x,y,r^{\hat{-}}) = \cos\left(\frac{\theta\,(xr^{\hat{-}})-\theta\,(yr^{\hat{-}})}{2}\right)\cos\left(\frac{\theta\,(r^{\hat{-}}-xr^{\hat{-}})-\theta\,(r^{\hat{-}}-yr^{\hat{-}})}{2}\right) \tag{13}$$

$$S(x,y,r^{\hat{-}}) = \sin\left(\frac{\theta(xr^{\hat{-}})-\theta(yr^{\hat{-}})}{2}\right)\sin\left(\frac{\theta(r^{\hat{-}}-xr^{\hat{-}})-\theta(r^{\hat{-}}-yr^{\hat{-}})}{2}\right).$$

Interestingly, in the light front limit, our interpolating bound state equation converges to the bound state equation in LFD which highlights the bridge between first principle QCD and the light front quark model. The backwards moving wave function $\hat{\phi}_-$ goes to zero in the LFD limit, and the $\hat{\phi}_+$ becomes the light-front bound state wave function. The meson mass spectra is then plotted in Fig.4 and shown to have the feature of Regge trajectories for the quark anti-quark bound states each with corresponding equal bare mass m. It is interesting to note the slight curvature differences found in the higher mass values. This result is consistent the Gell-Mann-Oakes-Renner relation in the chiral limit ($m \to 0$). We used these interpolating bound state wave functions to calculate alternative quasi-parton distribution functions (quasi-PDFs) implementable in lattice QCD calculations seen in [1]. These quasi-PDFs are dependent on both the momentum and our interpolation angle parameter.

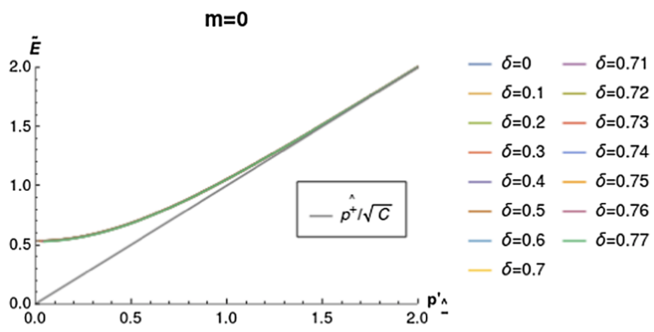

(a)

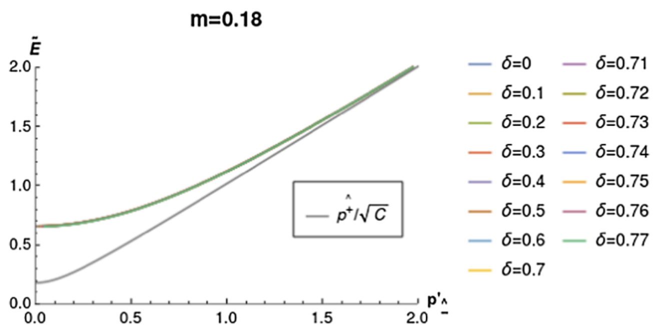

(b)

Figure 3: Mass gap solution plotted for light quarks m=0 and m=0.18

If we tune this angle close to the light front limit ($\delta = \frac{\pi}{4}$), we can obtain an accurate approximation for the light-front PDF that can be implemented on the lattice seen in Fig.5. We hope in future work, these interpolating quasi-PDFs will serve as a useful alternative to traditional quasi-PDFs, which are frequently used in the lattice QCD computations.

5. Conclusion and Future Work

We have interpolated the 't Hooft model between the instant form dynamics (IFD) and the light-front dynamics (LFD) using an interpolation angle parameter δ in the interpolating axial gauge. Using interpolation between IFD and LFD, we may be able to resolve the $\pi^0 = 0$ issue of the axial gauge in IFD as illustrated in Fig.1. We also plan to repeat the calculations done in the interpolating axial gauge using the interpolating Coulomb gauge. We expect that the route taken to obtain these physical quantities (like the constituent quark mass seen in Fig.3) will be different, but the obtained physical results will ultimately remain unchanged due to gauge invariance. We have calculated the bound state wave equations which connect the first principle QCD with the light front quark model in [1]. We want to further explore this connection using the interpolating Coulomb gauge. Additionally, extending the interpolating dynamics to 3+1 and $N_c = 3$ needs to be explored to study confinement. Eventually, we would like to utilize the interpolating quasi-PDFs in lattice QCD calculations to prove their effectiveness and strengthen our argument as to why the interpolating dynamics should be investigated further.

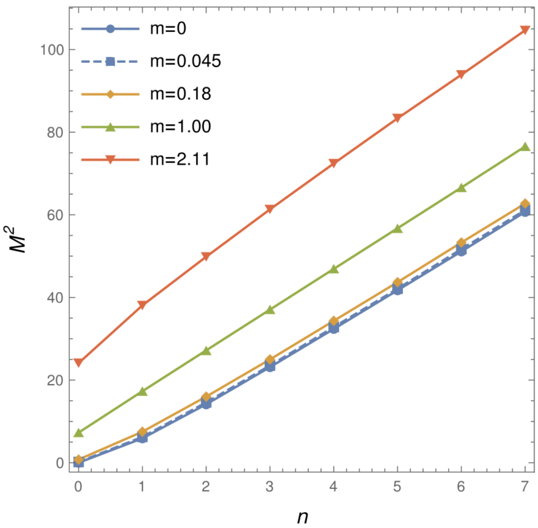

Figure 4: Meson mass spectra

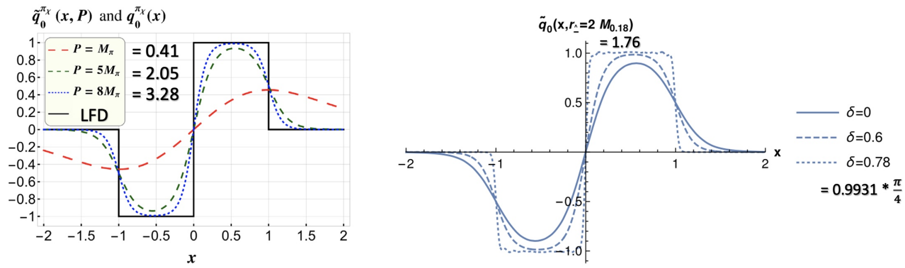

Figure 5: Interpolating quasi-PDF for the chiral pion compared with LFD PDF result in Minkowski space [11].

Acknowledgements

Acknowledgements : C.-R. Ji thanks Prof. Paul Hoyer for the useful discussions which motivated this work. This work was supported in part by the NCSU Provost's Professional Experience Program and the U.S. Department of Energy (Grant No. DE-FG02-03ER41260). The National Energy Research Scientific Computing Center (NERSC) supported by the Office of Science of the U.S. Department of Energy under Contract No. DE-AC02-05CH11231 is also acknowledged.

References

[1] B. Ma and C.-R. Ji, Phys. Rev. D104, 036004 (2021).

[2] P.A.M. Dirac, Rev. Mod. Phys. 21, 392 (1949).

[3] C.-R. Ji and C. Mitchell, Phys. Rev. D64, 085013 (2001).

[4] C.-R. Ji and A.T. Suzuki, Phys. Rev. D87, 065015 (2013).

[5] C.-R.Ji, LNP 1012, 2024 Springer Nature. (2023).

[6] G. ’t Hooft, Nucl. Phys. B75, 461 (1974).

[7] I.Bars and M.B.Green, Phys. Rev. D17, 537 (1978).

[8] P. Hoyer, arxiv, arXiv:2101.06721, (2021).

[9] C.-R. Ji, Z.Li and A.T. Suzuki, Phys. Rev. D 91, 065020 (2015).

[10] D. Zwanziger, vol. 131. Oxford University Press (OUP), pp. 233–242, (1998).

[11] Y. Frishman, C.T. Sachrajda, H. Abarbanel, and R. Blankenbecler, Phys. Rev. D 15, 2275 (1977).